



Original paper

Accurate non-tumoral ^{99m}Tc -MAA absorbed dose prediction to plan optimized activities in liver radioembolization using resin microspheres

Philippe d'Abadie*, Stephan Walrand, Michel Hesse, Nadia Amini, Renaud Lhommel, Kiswendsida Sawadogo, François Jamar

Cliniques Universitaires Saint-Luc Institut Roi Albert II, Brussels, Belgium



ARTICLE INFO

Keywords:

Radioembolization
Dosimetry
Partition model
 ^{99m}Tc -MAA SPECT/CT
 ^{90}Y PET/CT

ABSTRACT

Aim: The manufacturers' recommended methods to calculate delivered activities in liver radioembolization are simplistic and only slightly personalized. Activity planning could also be based on a ^{99m}Tc -macroaggregated albumin SPECT/CT (MAA) using the partition model but its accuracy is controversial. This study evaluates the dose parameters in the normal liver and in the tumor compartments using MAA SPECT/CT (pre-therapeutic imaging) and ^{90}Y TOF-PET/CT (post-therapy imaging). Finally, we propose a prescription of the activity as a function of the normal liver MAA distribution.

Method: 66 procedures of RE (with resin microspheres) corresponding to 171 lesions were analyzed. Tumor to normal targeted liver uptake (T/NTL), tumor absorbed dose (TD) and whole normal liver absorbed (WNLD) were assessed with MAA and ^{90}Y imaging. Secondly, activities were recalculated using the MAA distribution in the normal liver compartment to reach the maximal tolerable liver dose. These Activities were compared to activities defined with the BSA method.

Results: Compared to ^{90}Y imaging, our study demonstrated an accurate estimation of the WNLD using MAA imaging (Pearson's $R = 0.97$, $p < 0.001$). On the contrary, significant variations were found for TD ($R = 0.65$, $p < 0.001$). The MAA T/NTL ratio has a 85% positive predictive value in identifying patients who will get a ^{90}Y T/NTL ratio above 1.5. Moreover, activities calculated using the MAA distribution in the normal liver compartment were significantly higher to activities defined with the BSA method.

Conclusion: Whole normal liver absorbed doses are accurately predicted with MAA imaging and could be used to optimize the activity planning.

Introduction

Liver radioembolization (RE) is one of the available treatments for unresectable primary and secondary liver malignancies. The aim of treatment optimization is to deliver an efficient absorbed dose to tumors while keeping the absorbed dose to the non-tumoral liver parenchyma low enough in order to avoid a liver toxicity [1]. International authorities (i.e. Euratom 2013/59 and ICRP 140) require optimization of therapy through dose planning [2,3].

Before treatment, a first arteriography is performed for mapping the arterial tumor vascularization, for (a) prophylactic coil embolization(s) of small arterial branches oriented to the digestive tract and finally for simulating treatment with ^{99m}Tc -macroaggregated albumin (MAA) particles [4]. Following this, MAA nuclear imaging with SPECT/CT is performed for lung shunt estimation, for ruling out gastro-intestinal

deposition and in some centers for dosimetry planning [5,6]. After the RE, absorbed dose in the tumor and in the normal liver tissue can be assessed accurately with ^{90}Y Time-of-Flight (TOF)-PET/CT [7].

The manufacturers' recommended methods to calculate the activities to be delivered (specified in the package inserts) are simplistic and only slightly personalized. The body surface area (BSA) method is the most commonly used for ^{90}Y resin spheres (Sir-Spheres®, Sirtex Medical Ltd., Sydney, Australia) whereas some centers also use a compartmental model. A mono-compartmental model with a target liver absorbed dose of 80–150 Gy is used for ^{90}Y glass microspheres (Therasphere®, Boston Scientific, Boston, Massachusetts) and a maximal whole liver absorbed dose of 60 Gy for ^{166}Ho poly-L-lactic-acid (PLLA) microspheres (QuiremSpheres®, Quirem Medical B.V., Deventer, The Netherlands). These methods do not provide accurate dosimetry that separately takes into account the dose deposition in tumors and in the normal liver

* Corresponding author.

E-mail address: philippe.dabadie@uclouvain.be (P. d'Abadie).

<https://doi.org/10.1016/j.ejmp.2021.07.032>

Received 15 February 2021; Received in revised form 23 July 2021; Accepted 28 July 2021

Available online 23 August 2021

1120-1797/© 2021 Associazione Italiana di Fisica Medica. Published by Elsevier Ltd. All rights reserved.

parenchyma for a dose optimization as requested by the article 56 of the EEC Directive 2013/59 [2].

With resin microspheres and the BSA method, patients with a small liver might be overdosed and others with a large liver might be underdosed [8]. In addition, Kafrouni et al. demonstrated that the activity calculated with the BSA method was associated with a suboptimal absorbed dose to tumor and normal liver, under the usual cut-offs for tumor response and liver tolerance in HCC patients (i.e. 120 Gy and 50 Gy) [9]. Previous data also demonstrated that the delivered activity with the BSA method must be significantly reduced for patients with small liver (<1.5L) or with low tumor involvement (<5%) to avoid RE Induced Liver Disease (REILD) [10,11].

To overcome these issues, some centers have adopted a more personalized dosimetric method based on the MAA distribution in the tumor and the normal liver compartments known as the partition model [4]. This dosimetric method is considered to be more accurate and enables to plan a safe absorbed dose to the normal liver and an effective absorbed dose to tumors [12]. However, this model assumes a perfect correlation between MAA particles and the actual distribution of the radioactive ⁹⁰Y microspheres; this consideration is questionable and subject to debate. Indeed, previous studies demonstrated heterogeneous results in the ability of MAA imaging to precisely determine the tumor doses [13–15].

The aim of this study is to provide an optimized dosimetric method for activity planning in liver radioembolization with resin microspheres. For this purpose, we evaluated the accuracy of a dosimetric model based on MAA imaging. We compared tumor absorbed dose (TD) and whole normal liver absorbed dose (WNLD) calculated with MAA and ⁹⁰Y datasets in procedures realized in similar arteriographic conditions. As a second endpoint, we aim to propose a more accurate dosimetric model based on the MAA absorbed dose in the normal liver compartment. In this model, the injected radioactivity was calculated to reach the maximal absorbed dose tolerated by the normal liver without severe toxicity.

Material and methods

Patients and procedures

Patients treated by RE with resin microspheres between 2011 and 2019 were retrospectively analyzed after approval of the local ethics committee (2017/27JUI/334). Each treatment was performed according to the standards of clinical practice [4].

Characteristics of each arteriography were firstly reviewed by a senior interventional radiologist with a systematic analysis of the catheter tip position using the 2D angiography. Only patients with angiograms with similar catheter positions (difference < 1 cm) and comparable catheter positions (range 1 to 2 cm) between the preliminary and the therapeutic angiographies were included in this study. No other exclusion criteria were applied in this study.

Imaging protocols

^{99m}Tc-MAA imaging was performed after injection of 150 to 170 MBq ^{99m}Tc-MAA (Technescan LyoMAA, Mallinckrodt Medical BV, The Netherlands), using a Brightview XCT scanner (Philips Healthcare, Cleveland, OH). Abdominal SPECT/CT images were obtained with a 128x128 matrix with a low energy, high-resolution collimator (64 angles per head, 25 sec /angle). Image reconstruction was achieved using an OSEM algorithm (8 iterations and 16 subsets) with attenuation and scatter corrections.

⁹⁰Y imaging was realized with a 650 ps TOF-PET/CT (Gemini Time-Of-Flight-PET/CT, Philips Medical Systems, Cleveland, OH) with an abdominal acquisition of 40 min (2 bed positions). Reconstruction was performed with the 3-D line of response (LOR)-TOF blob-based algorithm (2 iterations, 33 subsets) and with a voxel reconstruction of 4x4x4

mm³.

Tumor uptake and grading

Small tumors with a volume under 4 ml (i.e. <2 cm diameter) were excluded from the analysis. For each lesion, the tumor to normal targeted liver uptake ratio (T/NTL) was defined as:

$$T/NTL = \frac{C_T/V_T}{C_{NTL}/V_{NTL}}$$

where C_T and V_T represent the counts and volume of each individual tumor, respectively. C_{NTL} and V_{NTL} represent the counts and volume of the normal targeted liver, respectively. NTL is the non-tumoral liver receiving radioactive microspheres (example in Fig. 1). C_T and C_{NTL} were measured with ^{99m}Tc-MAA SPECT and ⁹⁰Y PET datasets.

T/NTL was classified as low grade uptake for value less than 1.5 and as high grade for value higher or equal than 1.5.

Absorbed dose

Absorbed doses (D_{VOI}) have been determined using the MIRD equation [16], i.e.:

$$D_{VOI}(Gy) = \frac{A_{VOI}(GBq)}{M_{VOI}(kg)} \cdot 50(J/GBq)$$

where A and M are the activity and the mass within the VOI, respectively.

VOIs were first delineated using the baseline contrast enhanced MRI or CT scan using MIM 6.7 (MIM Software Inc., Cleveland, OH). Afterwards, MRI/CT scans and VOIs were fused with ^{99m}Tc-MAA SPECT and ⁹⁰Y PET using a rigid co-registration in order to measure the activity in the VOI.

Tumor absorbed dose (TD) and whole normal liver absorbed dose (WNLD) were calculated with ^{99m}Tc-MAA SPECT and ⁹⁰Y PET.

Calculations of activities using different dosimetric methods

In our cohort, we recalculated the activities needed for treatments of our 66 patients using the VOIs as defined above.

First, we calculated activities based on the BSA method (A_{BSA}) following the standard formula [17]:

for a whole liver treatment,

$$A(GBq) = BSA(m^2) - 0.2 + \frac{V_{tumor}}{V_{totalliver}}$$

for a treatment considering a part of the liver (target),

$$A(GBq) = \left((BSA(m^2) - 0.2) + \frac{V_{targettumor}}{V_{targetliver}} \right) \times \frac{V_{targetliver}}{V_{totalliver}}$$

where A is the activity, V, the volume and BSA, the body surface area defined as:

$$0.20247 \times height^{0.725}(m) \times weight^{0.425}(kg)$$

Secondly, activities were calculated from MAA imaging (A_{MAA}) using a two-compartment dosimetry model [6]. The injected radioactivity was calculated to reach the maximal absorbed dose tolerated by the normal targeted liver (NTLD) without expecting severe toxicity. The absorbed dose applied to the NTL was 50 Gy. A more aggressive target absorbed dose of 70 Gy was given for treatments only in patients with a functional liver reserve above 30% (percentage of non irradiated liver) and without risks of impaired liver function (underlying liver disease, previous hepatotoxic treatments). The formula was derived from the MIRD equation [16]:

$$A_{MAA}[GBq] = \frac{(C_{NTL}/C_{NTL})NTLD[Gy] \cdot M_{NTL}[kg] \cdot (1+LSF)}{50}$$

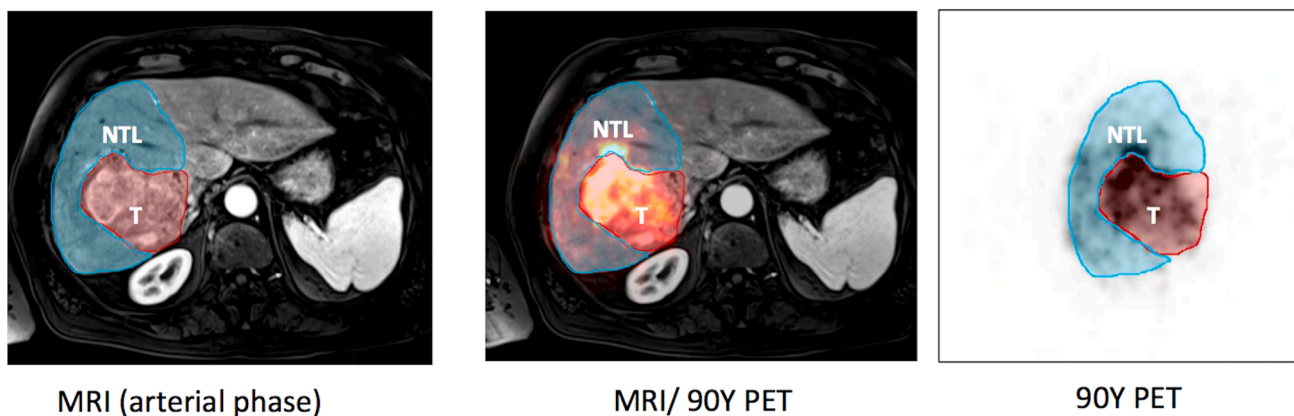


Fig. 1. Example of a patient with a large hepatocellular carcinoma shown on MRI (left panel). T represents the tumor and NTL, the normal targeted liver. The liver distribution of ⁹⁰Y-microspheres is assessed by ⁹⁰Y PET (right panel), fused with MRI (middle panel).

with C_{WL} and C_{NTL} , the counts defined with ^{99m}Tc-MAA SPECT in the whole liver and in the normal targeted liver (NTL) respectively; with NTLD the Maximal absorbed Dose tolerated by the NTL (50 or 70 Gy) and with M_{NTL} , the mass of the NTL. LSF is the lung shunt fraction estimated from planar images of the ^{99m}Tc-MAA scintigraphy.

Thirdly, we recalculated activities reaching the maximal tolerable whole normal liver absorbed dose (WNLD) of 40 Gy. The formula was also derived from the MIRD equation:

$$A_{MAA} [GBq] = \frac{(C_{WL}/C_{NTL})WNLD[Gy].M_{WL}[kg].(1 + LSF)}{50}$$

Statistics

Analyses were conducted by a senior statistician using SAS V9.4 software (SAS Institute Inc., Cary, NC, USA). Descriptive statistics were used to summarize the results considering absolute and relative frequencies, medians and absolute median deviations. Log base 10 was used for plotting lognormal distributions. Differences between ⁹⁰Y and MAA absorbed doses were analyzed using Bland-Altman plot. Variances of the differences between the tumor doses and between the whole normal liver absorbed doses were compared with a Brown and Forsythe's test. The correlation between parameters was also evaluated by a Pearson coefficient.

Wilcoxon rank sum test for paired data was used to analyze the differences in T/NTL and absorbed doses between ⁹⁰Y and MAA and to analyze the difference in planned activities between the classic BSA method and the two-compartment dosimetry method.

A linear mixed-effect model was used to account for correlation of tumors within patients.

The performance of MAA imaging to predict T/NTL, was assessed using the ⁹⁰Y imaging as gold standard. Sensitivity, specificity, accuracy, negative and predictive values were calculated as usual.

A P-value with a confidence level of 95% was defined as statistically significant.

Results

66 patients corresponding to 66 procedures of planning (with MAA imaging) and treatment (with ⁹⁰Y imaging) are reported in this study. Angiograms were classified similar (delta < 1 cm) and comparable (delta: 1 → 2 cm) in 48 and 18 procedures, respectively.

Main characteristics of patients and procedures are reported in Table 1. In summary, patients were treated mostly for hepatocellular carcinoma (HCC, 33%), colorectal metastases (32%) and for neuroendocrine tumors metastases (24%). 171 lesions were analyzed corresponding to an average of 3 lesions per patient. Lobar radioembolization

Table 1 Patient characteristics.

Characteristics		
Gender (n, %)	Female	22 (33%)
	Male	44 (67%)
Age (median- range; years)		67 (34–83)
Tumor type by patient (n, %)	HCC	22 (33%)
	Colorectal mets	21 (32%)
	Neuroendocrine mets	16 (24%)
	Cholangiocarcinoma	3 (5%)
	Melanoma mets	3 (5%)
	Oesophagus mets	1 (1%)
	Liver target for planning or treatment (n; %)	Whole liver
	lobar	35 (53%)
	Selective	2 (3%)
Number of lesions*		171
Number of lesions per patient (median- range)		3 (1–11)
Tumor volume (median; ml)		23.5 (4.2–1312)

mets: metastases; HCC: hepatocellular carcinoma
* only lesions with a diameter >2 cm were included

was performed in 53%, whole liver treatment in 44% (mostly by bilobar injection) and selective in only 3%. At the time of treatment, the activity that was actually injected was defined using the BSA method in 54 procedures (82%) and the partition dosimetric method in 12 (18%).

The estimates of the whole normal liver dose using MAA imaging (Figs. 2 and 3; Table 2) were highly accurate. The correlation between MAA and ⁹⁰Y whole normal liver doses was very strong (R = 0.97, p < 0.001) with a median absolute deviation of only 1.9 Gy. The maximum relative deviation from the linear fit was 29.6%. This variation was <5% for 39 patients (59%), <15% for 56 patients (85%) and <25% for 63 patients (95%). Bland-Altman plot (Fig. 3) demonstrated also that in 95% of cases, whole normal liver doses calculated with ⁹⁰Y imaging were 21.2% below and 20.6% above whole normal liver doses calculated with MAA imaging (0.788–1.206; 95% limits of agreement). For example, for a WNLD of 50 Gy calculated with MAA imaging, the real WNLD evaluated with ⁹⁰Y imaging could be between 39 Gy and 60 Gy with 95% confidence.

For tumor absorbed doses, the correlation was less precise (R = 0.65, P < 0.001) with quite significant differences between ⁹⁰Y and MAA doses (median absolute deviation 49.4 Gy; Figs. 2 and 3, table 2). Bland-Altman analyses (Fig. 3) demonstrated that in 95% of cases, tumor absorbed doses calculated with ⁹⁰Y imaging were 74.6% below and up to 4.5 times above tumor absorbed doses evaluated with MAA imaging (0.254–4.485; 95% limits of agreement). For example, for a TD of 100 Gy calculated with MAA imaging, the real (⁹⁰Y) TD could be between 25 and 450 Gy with 95% confidence. The linear mixed-effects regression

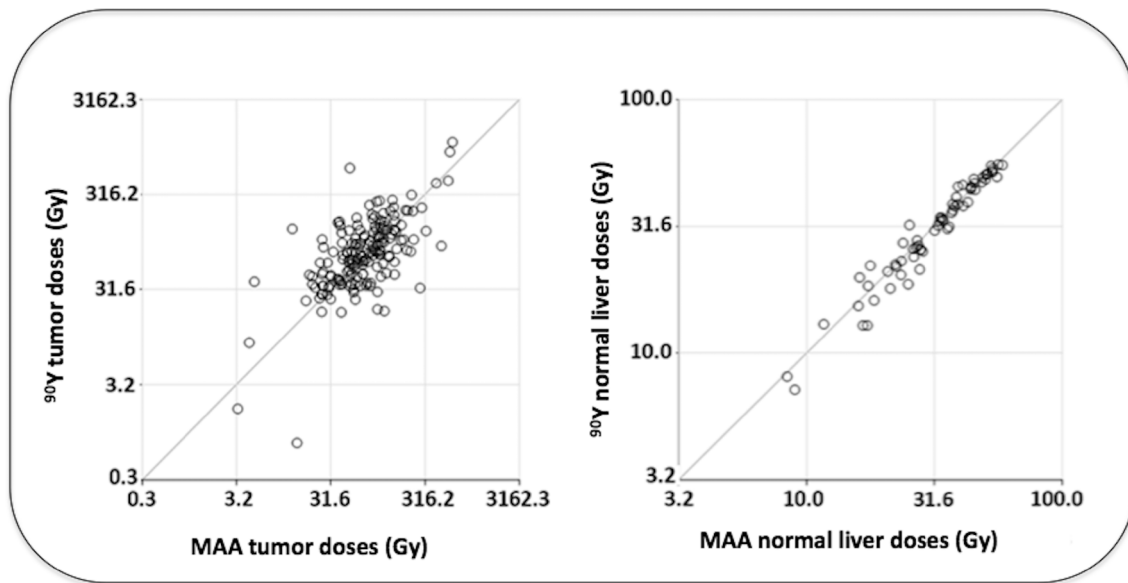


Fig. 2. Relation between ^{99m}Tc-MAA and ⁹⁰Y absorbed doses (Log 10), determined in tumors (n = 171; left panel) and in whole normal livers (n = 66; right panel).

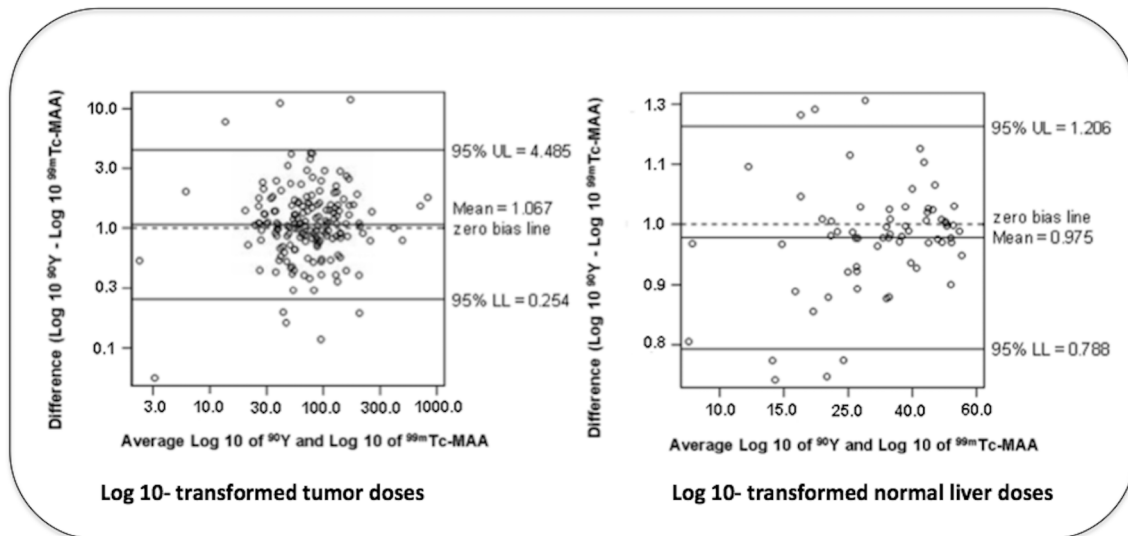


Fig. 3. Bland-Altman plots of log 10-transformed tumor absorbed doses (left panel) and log 10-transformed whole normal liver absorbed doses (right panel).

model showed a intraclass correlation coefficient of 0.37 meaning that measurements within patients were no more similar than measurements from different patients.

No significant differences were found for procedures realized in similar or comparable catheter positions (median absolute deviation: 47.8 Gy vs 55.1 Gy; table 2). The differences between ⁹⁰Y and MAA tumor absorbed doses were substantial for each tumor type (table 3).

The T/NTL grade was well predicted with MAA imaging using ⁹⁰Y imaging as gold standard (table 4). The low or high grades were predicted with a sensitivity of 77.6%, a specificity of 70.9%, a positive predictive value of 84.9% and a negative predictive value of 60%. In other words, MAA imaging was able to predict a high T/NTL uptake in 85%. Moreover, T/NTL calculated with ⁹⁰Y imaging was statistically higher to T/NTL calculated from MAA imaging (table 5).

The comparison between the BSA method and the two-compartment dosimetry method demonstrated significant differences in planned activities. Activities determined with the two-compartment dosimetry method were significantly higher than activities calculated with the BSA method using the different thresholds of whole or targeted normal liver

absorbed doses (table 6 and Fig. 4). Using a threshold of 50 or 70 Gy in the normal targeted liver, the injected activity would have been increased by more than 30% in 22 procedures (33%) and decreased by more than 30% in 2 procedures (3%), by comparison with the BSA method.

Discussion

In external beam radiation therapy (EBRT), dose planning is a very important step before treatment, and includes performing a segmentation of the tumor and surrounding healthy tissues, and evaluating their dose distribution [13]. This planning aims to deliver an efficient absorbed dose to the tumor while minimizing the absorbed dose to the adjacent organs, avoiding radiation induced morbidity [18]. Compared to EBRT, dosimetry in ⁹⁰Y-RE is not fully developed yet and only MAA SPECT/CT is currently available for dose simulations.

In our study, MAA imaging predicted with accuracy the whole normal liver absorbed dose, in agreement with recent studies [14,15,19]. Based on this knowledge, the activity could be planned

Table 2
Variability of the differences between ⁹⁰Y and ^{99m}Tc-MAA absorbed doses in tumors and whole normal liver according to the catheter position.

Factor			Tumor	whole normal liver	p-value [§]	
Difference between ⁹⁰ Y and ^{99m} Tc-MAA absorbed doses (90Y – ^{99m} Tc-MAA doses)	similar and comparable catheter positions	n	171	66		
		Mean (Gy)	10.9	– 0.6		
		Standard deviation (Gy)	89.34	2.69		
		Median (Gy)	3.7	– 0.5	0.153	
		Median absolute deviation (Gy)	49.4	1.9	< 0.001*	
		n	127	48		
	Similar catheter positions	Mean (Gy)	9.6	– 0.6		
		Standard deviation (Gy)	82.72	2.53		
		Median (Gy)	4.7	– 0.7	0.081	
		Median absolute deviation (Gy)	47.8	1.8	< 0.001*	
		Comparable catheter positions	n	44	18	
			Mean (Gy)	14.6	– 0.3	
Standard deviation (Gy)	107.18		3.13			
Median (Gy)	– 1.1		0	0.883		
Median absolute deviation (Gy)	55.1		2.2	< 0.058		

[§] : Wilcoxon signed rank test for comparing medians and Brown and Forsythe's Test for homogeneity of variance.
* : Indicates a significant p-value at the 5% threshold

accurately and safely, reaching the maximal tolerated absorbed dose of the normal liver. In our study, the maximal variation of the WNLDM_{MAA} compared to the linear fit was 29.6% but for a large majority of patients, this variation was below 15% (56 patients, 85%).

Threshold doses for liver toxicity and especially for REILD were analyzed in previous studies. With resin microspheres, the parenchyma exposure should be kept below 50 Gy for whole liver treatment and 70 Gy for lobar radioembolization, with low and acceptable risks of toxicity under these thresholds [20]. The tolerable absorbed dose to the healthy liver could be higher for lobar treatment (e.g. 70 Gy), especially when the liver reserve was superior to 30%. With glass microspheres, Garin et al. found that a high healthy liver absorbed dose associated with a liver reserve inferior to 30% was a strong factor for severe liver toxicity [21]. Using a computational model, Walrand et al. demonstrated also a dose-toxicity relationship dependent of the targeted liver volume. The predicted normal tissue complication probability (NTCP) was reduced when two-thirds of the liver was targeted compared to a whole liver treatment [22]. However, the maximum tolerable whole normal liver dose in patients treated with resin microspheres is not precisely identified by a radiobiological model demonstrating the risk of liver decompensation in function of the whole liver non tumoral absorbed dose. Sangro et al. observed a REILD in 9 patients out of 33, who received a whole normal liver absorbed dose of 37 ± 12 Gy [11]. In 20 patients treated by a whole liver approach for metastatic lesions and receiving 40 Gy to the whole non-tumoral liver, Cremonesi et al. did not observe toxicity [23]. Strigari et al demonstrated also a 50% probability of liver toxicity (≥G2) with a whole normal liver absorbed dose of 52 Gy (95% CI, 44–61 Gy) with a dosimetry based on bremsstrahlung SPECT [1].

Table 3
Variability of the differences between ⁹⁰Y and ^{99m}Tc-MAA absorbed doses in tumors and whole normal liver according to the type of tumor.

Type			Tumor	Whole normal liver	p-value [§]	
Difference between ⁹⁰ Y and ^{99m} Tc-MAA absorbed doses (90Y – ^{99m} Tc-MAA doses)	Hepatocellular carcinoma	n	36	22		
		Mean (Gy)	– 3.6	0.6		
		Standard deviation (Gy)	98.4	2.98		
		Median (Gy)	4.4	0.0	0.706	
		Median absolute deviation (Gy)	63.1	2.4	0.001*	
		n	71	21		
	Colorectal metastases	Mean (Gy)	3.6	– 1.1		
		Standard deviation (Gy)	75.76	2.69		
		Median (Gy)	2.2	– 0.8	0.392	
		Median absolute deviation (Gy)	33.5	1.9	0.080	
		Neuroendocrine metastases	n	48	16	
			Mean (Gy)	37.3	– 1.6	
Standard deviation (Gy)	107.06		2.12			
Median (Gy)	23.1		– 0.8	0.093		
Median absolute deviation (Gy)	66.4		1.6	0.019*		

[§] : Wilcoxon signed rank test for comparing medians and Brown and Forsythe's Test for homogeneity of variance.
* : Indicates a significant p-value at the 5% threshold.

Table 4
Tumor to normal targeted liver (T/NTL) grades defined with ^{99m}Tc-MAA SPECT/CT and ⁹⁰Y PET/CT. Tumor grades were defined as low and high using a threshold of 1.5.

T/NTL	High grade ⁹⁰ Y (≥1.5)	Low grade ⁹⁰ Y (<1.5)
High grade _{MAA} (≥1.5)	90	16
Low grade _{MAA} (<1.5)	26	39

Table 5
Differences between ⁹⁰Y and ^{99m}Tc-MAA tumor to normal targeted liver uptake (T/NTL).

Factor	T/NTL MAA	T/NTL ⁹⁰ Y	p-value [§]
n	171	171	0.015*
Mean	2.59	3.09	
Standard deviation	2.840	4.320	
Median	1.80	1.84	
Minimum	0.09	0.02	
Maximum	20.94	41.69	

[§] : p-value from Wilcoxon rank sum test for paired data
* : Indicates a significant p-value at the 5% threshold

However, in this cohort of HCC patients, 15 of the 73 patients (20%) had advanced cirrhosis (Child B or more) and then a lower tolerability to radiations. Accordingly, recent international recommendations determined that the mean absorbed dose to the non-tumoral whole liver ≤ 40 Gy is considered safe [24]. Moreover, the liver tolerance to radiations

Table 6

Differences in activities retrospectively planned with the BSA method and with the two-compartment dosimetry method reaching different absorbed doses to the normal liver compartment.

Normal liver ^{99m} Tc-MAA absorbed dose		Activity BSA method (GBq)	Activity two-compartment dosimetry method (GBq)	p-value [§]
Normal targeted liver absorbed dose: 70 Gy	n	17	17	0.042*
	Mean	1.00	1.84	
	Standard deviation	0.390	1.400	
	Median	1.01	1.26	
	Minimum	0.48	0.62	
Normal targeted liver absorbed dose: 50 Gy	n	49	49	0.047*
	Mean	1.56	1.95	
	Standard deviation	0.430	0.910	
	Median	1.61	1.75	
	Minimum	0.29	0.35	
Normal targeted liver absorbed dose: 50 Gy or 70 Gy (all patients)	n	66	66	0.009*
	Mean	1.41	1.92	
	Standard deviation	0.490	1.050	
	Median	1.51	1.69	
	Minimum	0.29	0.35	
Whole normal liver absorbed dose: 40 Gy (all patients)	n	66	66	<0.0001*
	Mean	1.41	1.86	
	Standard deviation	0.490	1.120	
	Median	1.51	1.59	
	Minimum	0.29	0.82	
	Maximum	2.63	8.18	

* : Indicates a significant p-value at the 5% threshold. §: P value from Wilcoxon signed rank test for paired data.

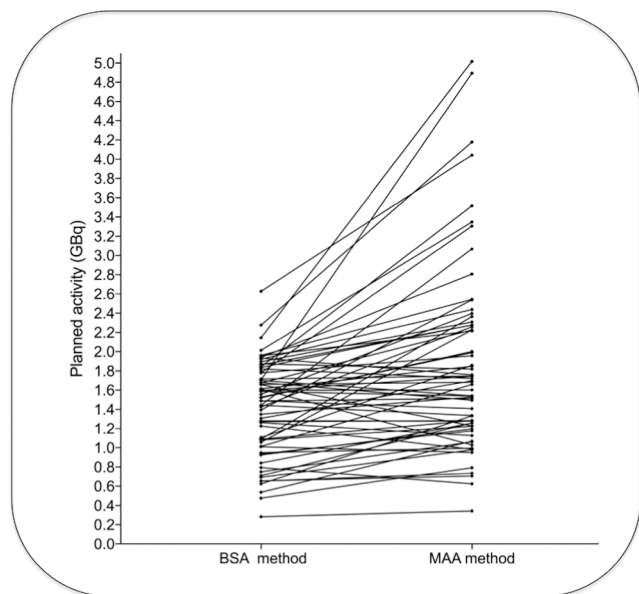


Fig. 4. Comparison of the planned activity defined with the BSA method and the two-compartment dosimetry method reaching the maximum tolerable absorbed dose to the normal targeted liver.

also differs as a function of the individual patient status. The liver tolerance is reduced in HCC patients as compared to metastatic liver patients [25]. Most of the HCC patients have an underlying liver disease (cirrhosis of any causes, chronic HBV,...) with an impaired hepatic

function, hence a lower tolerance to radiations. The stage of the liver disease is an important parameter and especially, an abnormal basal bilirubin ≥ 1.1 mg/dl or a Child-Pugh score B or C are strongly correlated with the occurrence of toxicity [26,27]. Previous hepatotoxic chemotherapies could also reduce the liver function reserve and the tolerance to radiations [28].

In comparison to the classic BSA method, the two-compartment dosimetry method developed here demonstrated the possibility to improve significantly the planned activity in many cases, expecting an increase in tumor absorbed dose and hence in tumor control probability [1]. In our cohort, using a simulation in the normal targeted liver compartment, tumor absorbed doses were significantly higher with the two-compartment dosimetry method than tumor absorbed doses estimated with the BSA method (median ⁹⁰Y TD: 93 Gy vs 76 Gy, $p < 0.001$). In HCC patients, a tumor absorbed dose greater or equal to 100 Gy was associated with higher tumor control and longer survival in a secondary analysis of the prospective SARAH study [29]. In our data, the absorbed dose threshold of 100 Gy was achieved in 31 of the 47 tumors (66%) with the two-compartment dosimetry method and in only 24 tumors (51%) using the BSA method. The activity planned with BSA method could result in low tumor absorbed doses. This might explain the negatives results of previous prospective trials [30,31]. Moreover, in a few patients of our study, activity planned with the two-compartment dosimetry was lower by comparison with the activity delivered by the BSA method. Previous studies have confirmed the risks of overdosing using the BSA model, especially for patients with small livers or with limited tumor involvement [8,10,11]. As suggested by some previous data [9,32], our results support to abandon the BSA method for activity planning with resin microspheres for a more optimized method based on the two-compartment dosimetry model.

In our study, we defined two models of activity planning based on the MAA non-tumoral distribution. A first model targeted the maximum non-ablative absorbed to the normal targeted liver and the second model targeted the maximum tolerable absorbed dose to the whole non-tumoral liver. This second approach was recently suggested by Chiesa et al., in order to improve the treatment planning [27]. In this study, the absorbed dose averaged over the whole non-tumoral liver was a strong risk factor for liver decompensation. In this large cohort of HCC patients treated with glass microspheres, a 15% liver decompensation risk (NTCP analysis) was associated with a non-tumoral whole liver absorbed dose of 90 Gy, or 50 Gy for patients with increased bilirubinemia (bilirubin >1.1 mg/dl). Previously, Strigari et al. defined also a strong relationship between the risk of liver toxicity and the whole normal liver absorbed dose in HCC patients treated with resin microspheres [1]. In EBRT, the absorbed dose averaged over the whole normal liver is also the strong predictor of radiotherapy induced liver disease [33]. Moreover, Dawson et al. analysed the correlation between the liver tolerance to radiations and the proportion of the irradiated liver volume [25]. Using the Lyman NTCP model, they demonstrated that the liver tolerance was inversely proportional to the irradiated liver fraction. In other words, the absorbed dose to the irradiated normal liver could be increased when the irradiated volume proportion decreases, without higher risks of liver decompensation. Therefore, the activity planning based on the WNLD is the most optimized method permitting to deliver the maximal tolerable activity. In regards with this radiobiological approach, a dose limitation on the normal targeted liver is unnecessary to avoid a REILD. However, the two-compartment dosimetry method using a WNLD approach could result in significant effects in the normal targeted liver especially when the targeted volume is relatively small as compared to the whole liver volume (high normal targeted liver absorbed dose). Besides, a lobar normal liver absorbed above 70 Gy with resin microspheres could be ablative (radiation lobectomy) [24]. Local toxicity can be expected such as cholangitis, biloma and fibrosis [34–36]. Moreover, due to the high number of microspheres per GBq, a high activity of resin microspheres injected in a small volume increases the risk of vascular saturation, flow stasis and reflux in non-targeted tissues [37]. Therefore, this method is

not the preferable approach when a small proportion of the liver volume is irradiated (i.e. < 40%), to avoid a local toxicity (other than liver decompensation).

With regards to the tumor absorbed doses, significant variations between the planned dose (MAA imaging) and the real dose (^{90}Y imaging) were demonstrated in our study. This variability was sometimes very substantial despite a similar catheter placement between the preliminary and therapeutic arteriographies. However, many other angiographic parameters could influence the particles' delivery by the catheter and generate local differences in the liver distribution [38]. This tumor absorbed dose approximation demonstrates the lack of accuracy of MAA imaging for dose planning in the tumor compartment. Recent recommendations purposed a personalised approach reaching an efficacy tumor absorbed dose cut-off of 100–120 Gy for HCC using $^{99\text{m}}\text{Tc}$ SPECT/CT [24]. Indeed, using the partition model, the activity prescription consists in delivering a target tumor absorbed dose while preserving the liver parenchyma by a safety absorbed dose to the normal liver compartment. However, previous radiobiological analyses demonstrated a continuous relationship (sigmoid shape) between the tumor absorbed dose and the tumor control probability [1,29]. In our MAA model, we would reach the maximum tolerable activity and then the maximum absorbed dose to tumor to reach the maximal probability of tumor control.

Regarding our analysis of the tumor absorbed dose, MAA imaging was not very accurate with a risk of underestimation or overestimation (table 2, Fig. 2 and Fig. 3). Moreover, the grade of tumor to normal liver targeted uptake (T/NTL) could be misestimated. Nevertheless, a T/NTL at least 1.5 fold higher than the normal targeted liver was well predicted in 85% (table 5). Therefore, a high tumor absorbed dose (i.e. a high T/NTL) was well predicted in most cases and could explain the good clinical results of previous studies using a dosimetry performed with MAA imaging and using a threshold tumor absorbed dose [29,39]. Using the two-compartment dosimetry method reaching the maximal tolerable absorbed dose to the targeted normal liver (50 Gy or 70 Gy), the MAA tumor absorbed doses and the ^{90}Y tumor absorbed doses could be recalculated in our 47 HCC tumors. Then, 28 on 47 tumors had a MAA tumor absorbed dose ≥ 100 Gy (60%) and 31 tumors (66%) reached this threshold dose in reality (^{90}Y imaging). The MAA threshold absorbed dose of 100 Gy defined by Hermann et al. was well predicted in 90% in this population of tumors [29]. Nevertheless, in our data, a low tumor absorbed dose (i.e. low T/NTL) could be underestimated with MAA imaging in a significant number of tumors (Table 4). Therefore, RE should not be withheld in all cases when the efficacy absorbed dose cut-off is not reached with the partition model.

Previously, in a large cohort of patients, Ilhan et al. found more discordance between $^{99\text{m}}\text{Tc}$ -MAA SPECT and ^{90}Y -bremsstrahlung SPECT tumor uptakes using a visual scale [40]. This difference could be explained by the lower image quality of ^{90}Y -bremsstrahlung SPECT compared to ^{90}Y -TOF-PET systems [41]. In accordance with our study, some previous data showed also a trend of MAA imaging to underestimate the actual absorbed dose [14,42,43]. However, Gnesin et al. demonstrated the opposite in a serie of HCC patients and Kafrouni et al. identified only minimal differences especially when the catheter position was deemed identical between procedures [15,44].

Our results have to deal with several limitations. Firstly, a threshold of 2 cm between the catheter tip positions was used for patient inclusion in this study. However, unnoticeable differences in catheter tip positions (e.g. 5 mm) could be responsible for important variations in particle distributions in segment-to-segment distribution and explain some differences in tumor absorbed doses [45]. Secondly, this dosimetry was realized with a rigid co-registration of SPECT and PET images with the baseline enhanced CT scan or MRI. Due to physiological liver deformations and differences in spatial resolution between imaging techniques, some misalignments could occur and lead to variations in absorbed dose calculations [46]. Future developments in deformable/elastic registration and its implementation in the workflow of

commercially available dosimetric softwares may improve the accuracy of the dose planning [47]. Thirdly, the activities based on MAA imaging were calculated with a correction for the lung shunt, using planar scintigraphic images. However, this lung shunt is significantly overestimated with planar images and could be more accurately predicted using SPECT/CT [48].

Fourthly, this study is retrospective: the activity choice through the two-compartment dosimetry model, reaching the maximum tolerable liver absorbed dose, needs to be validated in future studies. The lack of data that precisely determine the correlation between the whole normal liver absorbed dose and the risk of liver decompensation is a limitation for an application in clinical practice. Similarly to the previous works of Strigari et al. and Chiesa et al., only a NTCP analysis in a large cohort of patients would allow to clarify this risk using resin microspheres [1,27]. Moreover, additional dose-toxicity studies focused on local radiation damage are necessary to estimate the maximal absorbed doses tolerated by the targeted normal liver volume.

Conclusion

$^{99\text{m}}\text{Tc}$ -MAA SPECT dosimetry offers an excellent prediction of the whole normal liver absorbed dose. $^{99\text{m}}\text{Tc}$ -MAA SPECT/CT could be used in practice to plan the injected activity reaching the maximal tolerable absorbed dose to the whole normal liver. With this approach, the radioembolization treatment planning would be better personalized and optimized, expecting more efficiency, while controlling the toxicity.

Declaration of Competing Interest

The authors declare that they have no known competing financial interests or personal relationships that could have appeared to influence the work reported in this paper.

Acknowledgements

We are very grateful to Aline Van Maanen from the Department of Biostatistics (Saint Luc University hospital and king Albert II cancer Institute) for her help in the statistical analysis.

References

- [1] Strigari L, Sciuto R, Rea S, Carpanese L, Pizzi G, Soriani A, et al. Efficacy and toxicity related to treatment of hepatocellular carcinoma with ^{90}Y -SIR spheres: radiobiologic considerations. *J Nucl Med* 2010;51(9):1377–85. <https://doi.org/10.2967/jnumed.110.075861>.
- [2] E. c. d. euratom. Basic safety standards for protection against the dangers arising from exposure to ionising radiation and repealing Directives 9/618/Euratom, 90/641/Euratom, 96/29/Euratom, 97/43/Euratom and 2003/122/Euratom. *OJ of the EU*, vol. L53;57, pp. 1-73, 2014.
- [3] ICRP. Radiological protection in therapy with radiopharmaceuticals. *Ann. ICRP* 48, vol. Publication 140, 2019.
- [4] Padia SA, Lewandowski RJ, Johnson GE, Sze DY, Ward TJ, Gaba RC, et al. Radioembolization of hepatic malignancies: background, quality improvement guidelines, and future directions. *J Vasc Interv Radiol*. 2017;28(1):1–15. <https://doi.org/10.1016/j.jvir.2016.09.024>.
- [5] Garin E, Rolland Y, Laffont S, Edeline J. Clinical impact of ($^{99\text{m}}\text{Tc}$ -MAA SPECT/CT-based dosimetry in the radioembolization of liver malignancies with (^{90}Y -loaded microspheres. *Eur J Nucl Med Mol Imaging* 2016;43(3):559–75. <https://doi.org/10.1007/s00259-015-3157-8>.
- [6] Ho S, Lau WY, Leung TWT, Chan M, Ngar YK, Johnson PJ, et al. Partition model for estimating radiation doses from yttrium-90 microspheres in treating hepatic tumours. *Eur J Nucl Med* 1996;23(8):947–52. <https://doi.org/10.1007/BF01084369>.
- [7] Lhomme R, van Elmbt L, Goffette P, Van den Eynde M, Jamar F, Pauwels S, et al. Feasibility of ^{90}Y TOF PET-based dosimetry in liver metastasis therapy using SIR-Spheres. *Eur J Nucl Med Mol Imaging* 2010;37(9):1654–62. <https://doi.org/10.1007/s00259-010-1470-9>.
- [8] Lam MG, Louie JD, Abdelmaksoud MH, Fisher GA, Cho-Phan CD, Sze DY. AbdelmaksoudMH, Fisher GA, Cho-Phan CD, Sze DY. Limitations of body surface area-based activity calculation for radioembolization of hepatic metastases in colorectal cancer. *J Vasc Interv Radiol* 2014;25(7):1085–93. <https://doi.org/10.1016/j.jvir.2013.11.018>.

